Journal of Biomolecular NMR **30:** 397–406, 2004.

Estimates of methyl ^{13}C and ^{1}H CSA values ($\Delta\sigma$) in proteins from cross-correlated spin relaxation

Vitali Tugarinov[a], Christoph Scheurer[b], Rafael Brüschweiler[c] & Lewis E. Kay[a]
[a]*Protein Engineering Network Center of Excellence, Departments of Medical Genetics, Biochemistry and Chemistry, University of Toronto, Toronto, Ont. Canada M5S 1A8;* [b]*Lehrstuhl für Theoretische Chemie, Technische Universität München, 85748 Garching, Germany;* [c]*Gustaf H. Carlson School of Chemistry, Clark University, Worcester, Massachusetts 01610, U.S.A.*

Received 14 July 2004; Accepted 28 September 2004

Key words: DFT, ^{1}H, ^{13}C methyl CSA, methyl groups

Abstract

Simple pulse schemes are presented for the measurement of methyl ^{13}C and ^{1}H CSA values from ^{1}H–^{13}C dipole/^{13}C CSA and ^{1}H–^{13}C dipole/^{1}H CSA cross-correlated relaxation. The methodology is applied to protein L and malate synthase G. Average ^{13}C CSA values are considerably smaller for Ile than Leu/Val (17 vs. 25 ppm) and are in good agreement with previous solid state NMR studies of powders of amino acids and dipeptides and in reasonable agreement with quantum-chemical DFT calculations of methyl carbon CSA values in peptide fragments. Small averaged ^{1}H CSA values on the order of 1 ppm are measured, consistent with a solid state NMR determination of the methyl group ^{1}H CSA in dimethylmalonic acid.

Introduction

The relaxation properties of methyl groups have been the subject of numerous theoretical and experimental studies (Werbelow and Marshall, 1973; Werbelow and Grant, 1977; Muller et al., 1987; Kay and Prestegard, 1987; Kay and Torchia, 1991; Palmer et al., 1991). The interest stems from the fact that methyls are outstanding probes of both molecular dynamics and structure. For example, some of the earliest studies of molecular dynamics by NMR focused on ^{13}C spin relaxation of methyl groups (Richarz et al., 1980) and much later the incorporation of ^{2}H into methyls to create $^{13}CH_2D$ spin systems has lead to the use of deuterium as a spin-spy probe of motions in proteins (Muhandiram et al., 1995; Millet et al., 2002; Skrynnikov et al., 2002). Because of their position at the ends of side chains that often point into the hydrophic cores of proteins, distances between proximal methyl groups are extremely valuable in structure studies (Metzler et al., 1996; Rosen et al., 1996; Gardner et al., 1997; Mueller et al., 2000;). Finally, methyl groups can be isotopically labeled in ways that can be optimized for the particular study in question; for example the production of highly deuterated, methyl protonated proteins (Goto et al., 1999) has been shown to be advantageous for the assignment of methyl groups in high molecular weight systems (Gardner et al., 1998; Tugarinov and Kay, 2003a) and for the determination of global protein folds (Mueller et al., 2000).

The dominant relaxation interactions in $^{13}CH_3$ groups derive from dipolar couplings between intra-methyl ^{1}H—^{1}H and ^{1}H—^{13}C spins (Werbelow and Marshall, 1973; Werbelow and Grant, 1977; Kay and Bull, 1992). The rich network of cross-correlated spin interactions that results can be put to good use in applications to high molecular weight proteins, where it has been recently shown that a methyl TROSY effect can be

exploited, leading to spectra of high resolution and sensitivity (Ollerenshaw et al., 2003; Tugarinov et al., 2003). The relaxation in methyl groups also derives from ^{13}C and ^{1}H chemical shielding anisotropies (CSAs), although such contributions are much smaller than those from dipolar interactions. Not surprisingly, there have been few experiments that quantify methyl relaxation in proteins due to CSA. Several solid state NMR studies have provided estimates of ^{13}C CSA values for methyl groups in amino acids (Ye et al., 1993; Ishima et al., 2001) along with at least one solution study (Liu et al., 2003) and ^{1}H methyl CSA values in a variety of small compounds, in general not related to amino acids, have been summarized (Duncan, 1990). Our goal in the present work is to supplement these studies by obtaining qualitative measures of chemical shielding anisotropies ($\Delta\sigma$) for both ^{13}C and ^{1}H spins in methyl groups in a pair of proteins, protein L (64 residues) and malate synthase G (MSG, 723 residues) using solution spin relaxation experiments.

Materials and methods

NMR samples

U-[^{15}N,^{2}H], Ileδ1-[$^{13}CH_3$], Leu,Val-[$^{13}CH_3$, $^{12}CD_3$]-labeled samples of the B1 immunoglobulin binding domain of peptostreptoccocal protein L (Scalley et al., 1997) and malate synthase G (MSG) (Howard et al., 2000; Tugarinov et al., 2002) were obtained as described previously using U-[^{2}H]-glucose and $^{15}NH_4Cl$ (CIL, Andover, MA) as the carbon and nitrogen sources, respectively (Tugarinov and Kay, 2003b; Tugarinov and Kay, 2004). The addition of 80 mg of 2-keto-3,3-d_2-4-^{13}C-butyrate and 120 mg of 2-keto-3-methyl-d_3-3-d_1-4-^{13}C-butyrate per L of growth media one hour prior to induction led to the production of perdeuterated proteins with protonation restricted to Ile δ1 methyls and one of the methyl groups of Leu and Val (Leu,Val-[$^{13}CH_3$,$^{12}CD_3$]). Sodium salts of 2-keto-4-^{13}C-butyric and 2-keto-3-methyl-d_3-4-^{13}C-butyric acids were obtained from Isotec (Miamisburg, OH), and the 3-[^{1}H] positions subsequently exchanged to ^{2}H according to Gardner and Kay (1997) and Goto et al. (1999). Both proteins were purified as described earlier (Mittermaier and Kay, 1999; Tugarinov et al., 2002). The NMR sample of protein L was 99.9% D_2O, 50 mM sodium phosphate buffer (pH 6.0, uncorrected), 1.4 mM in protein, while the sample of MSG was 0.9 mM in protein, 99.9% D_2O, 25 mM sodium phosphate buffer (pH 7.1, uncorrected), 20 mM $MgCl_2$.

NMR spectroscopy

NMR experiments were performed on Varian Inova spectrometers equipped with pulsed-field gradient triple resonance probes at 5 °C (for protein L) and 37 °C (for MSG). The intensity ratios of both outer and inner ^{13}C multiplet components in F_1-coupled ^{1}H—^{13}C CT-HSQC spectra (Santoro and King, 1992; Vuister and Bax, 1992) (pulse sequence of Figure 1a) of protein L were obtained from data sets recorded with parametrically varied delays T of 40, 50, 60, 70, 80, 90, 110, 150 ms at 500, 600 and 800 MHz spectrometer fields. Delays $T = 20$, 30, 40, 50, 60 ms were used in the same measurements performed on the sample of MSG at 800 MHz. Relaxation rates of the two methyl ^{1}H doublet components (pulse sequence of Figure 1b) of protein L were obtained using delays T' of 150, 200, 250, 300 ms at 500, 600 and 800 MHz, while delays $T' = 5$, 15, 25, 35, 45, 55, 65 ms were used for MSG (800 MHz). All NMR spectra were processed using the NMRPipe/NMRDraw suite of programs (Delaglio et al., 1995) and analyzed using Matlab v.6 software (MathWorks, Inc., MA).

DFT calculations

DFT calculations were performed on partially optimized peptide fragments including residues Ile30, Ile44, Leu15, Leu43, Val17, and Val26 taken from the NMR structure of ubiquitin 1D3Z (Cornilescu et al., 1998). Each of the fragments contained all backbone and sidechain atoms of the respective residue i and, additionally, the C′ and O atoms of residue $i - 1$ and the N and H^N atoms of residue $i + 1$. The fragments were saturated with hydrogen atoms replacing the C^α atoms of residues $i - 1$ and $i + 1$, respectively. As the focus of the DFT calculations used here was not on the exact representation of the methyl groups in their specific protein environments, but rather on general

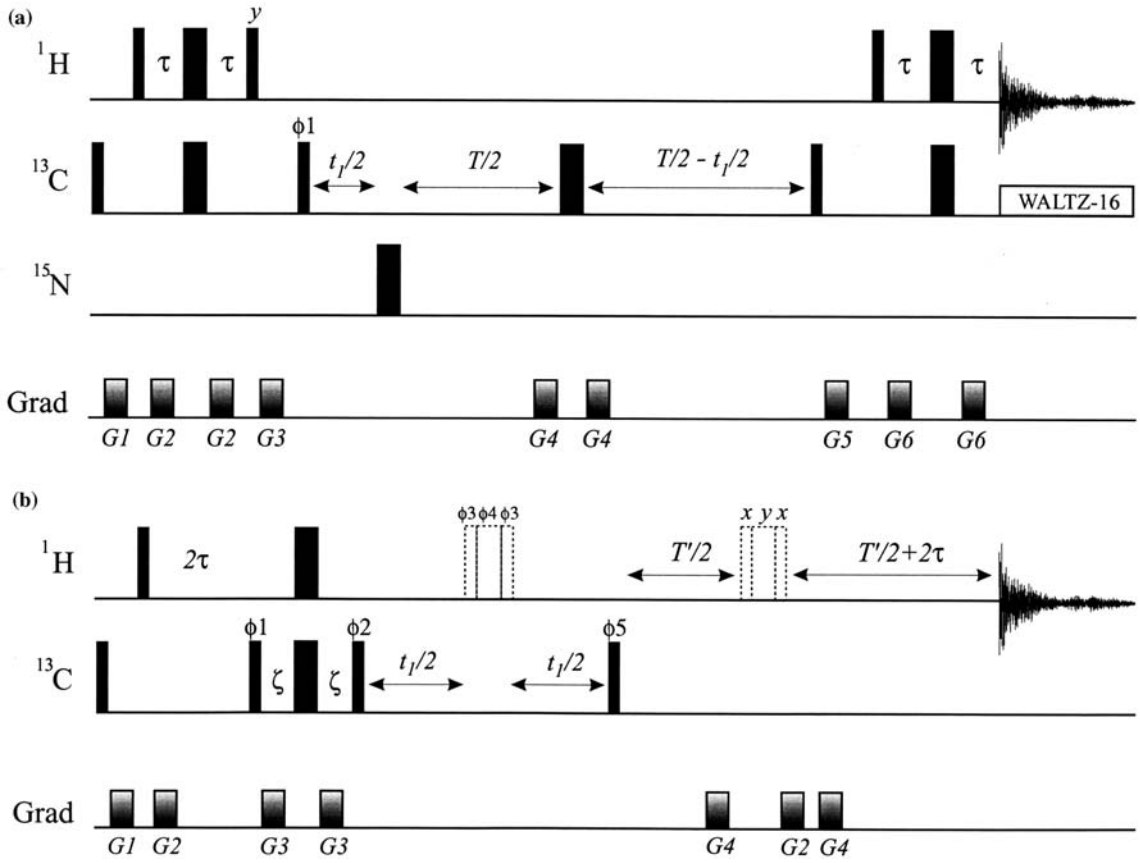

Figure 1. Pulse sequence used for the measurement of **(a)** methyl ^{1}H-^{13}C dipolar/^{13}C CSA cross-correlation rates and **(b)** methyl ^{1}H-^{13}C dipolar/^{1}H CSA cross-correlation rates as described in the text. All narrow (wide) rectangular pulses are applied with flip angles of 90° (180°) along the *x*-axis unless indicated otherwise. The ^{1}H and ^{13}C carriers are positioned in the center of the methyl region: 0.7–1.0 ppm and 18.5–19.0 ppm, respectively. All ^{1}H and ^{13}C pulses are applied with the highest available power with ^{13}C WALTZ-16 decoupling (Shaka et al., 1983) achieved using a 2 kHz field. The ^{1}H pulses shown with dashed lines are of the composite variety, 90°*x*–180°*y*–90°*x* (Levitt and Freeman, 1978). Delays: $\tau = 1.8$ ms, $\zeta = 1.0$ ms ($1/(8^1J_{HC})$). *T* and *T'* are parametrically varied delays (see text). **(a)** The durations and strengths of the pulsed field gradients applied along the *z*-axis are: G1 = (2.0 ms, 2.0 G/cm), G2 = (0.5 ms, 2.0 G/cm), G3 = (1 ms, 7.5 G/cm), G4 = (0.2 ms, 15 G/cm), G5 = (1 ms, −5 G/cm), G6 = (0.5 ms, 4 G/cm). The phase cycle is: ϕ1 = *x*,−x; rec. = *x*,−x. Quadrature detection in F_1 is achieved with States-TPPI incrementation of ϕ1 (Marion et al., 1989). **(b)** The durations and strengths of the pulsed field gradients applied along the *z*-axis are: G1 = (1.0 ms, 5.0 G/cm), G2 = (0.6 ms, 20 G/cm), G3 = (0.3 ms, −7.5 G/cm), G4 = (0.5 ms, 5 G/cm). The phase cycle is: ϕ1 = *x*,−x; ϕ2 = *4*(*y*),*4*(−y); ϕ3 = 2(*x*),*2*(*y*),*2*(−x),*2*(−y); ϕ4 = 2(*y*),2(−x),*2*(−y),*2*(*x*); ϕ5 = *x*; rec. = *x*,−x,−x,x. Quadrature detection in F_1 is achieved with States-TPPI incrementation of ϕ5.

aspects of sidechain methyl group CSAs, no partial charges or contact fragments representing the surrounding protein were included (Scheurer et al., 1999). The fragments were subsequently partially optimized with TURBOMOLE (version 5.5) (Ahlrichs et al., 1989; Ahlrichs and Arnim, 1995) at the B3LYP/TZVP level in internal coordinate representation, with the backbone φ, ψ, and ω angles as well as the sidechain χ angles fixed at their values from the NMR structure. The methyl groups were allowed to rotate around their respective C_{methyl}–C axes.

The CSA calculations were performed using the LOC1 SOS-DFPT approximation as implemented in the MASTER-CS module of deMon (Salahub et al., 1991; Malkin et al., 1995a), using the Perdew–Wang-91(PW91) functional (Perdew and Wang, 1992) and a FINE RANDOM angular grid with 64 radial shells for the integration. Basis functions from the IGLO-II basis set (Kutzelnigg et al., 1991) were used for all sidechain atoms, while the remaining atoms were treated with the DZVP basis set (Godbout et al., 1992; Sosa et al., 1992). Using larger basis sets or

an IGLO basis for all atoms in the fragment resulted in negligible changes in the computed CSA tensors.

The CSA tensors obtained from the DFT computations were symmetrized and subsequently diagonalized. CSA tensors for the three protons of each methyl were averaged prior to symmetrization and diagonalization. The values of σ were defined according to $\sigma_Z \geq \sigma_Y \geq \sigma_X$ and in all cases the angle between each principle axis of the tensor and the methyl three fold was smallest for the Z-axis.

Results and discussion

In order to quantify methyl ^{13}C chemical shielding anisotropies we have measured the contributions to the relaxation of methyl ^{13}C multiplet components arising from cross-correlation between ^{1}H–^{13}C dipolar and ^{13}C CSA interactions. Similar experiments have been employed for the measurement of dipole/CSA interference in ^{1}H–^{15}N (Tjandra and Bax, 1997b; Kroenke et al., 1998) and $^{1}H^{\alpha}$–$^{13}C^{\alpha}$ (Tjandra and Bax, 1997a) spin systems in proteins. In the present case ^{1}H–^{13}C CT HSQC correlation maps have been recorded, where the constant-time period during which ^{13}C evolution and relaxation occurs, T, is varied in a set of experiments, Figure 1a. All experiments have been performed on U-[^{2}H,^{15}N] Ileδ1-[$^{13}CH_3$], Leu,Val-[$^{13}CH_3$,$^{12}CD_3$] samples (Tugarinov and Kay, 2003b) of protein L (Scalley et al., 1997) and malate synthase G (Howard et al., 2000; Tugarinov et al., 2002). Because ^{13}C labeling is restricted only to methyl positions, values of T can be adjusted to optimize differences in multiplet component intensities and hence measurement of cross-correlation relaxation rates, without concern about ^{13}C–^{13}C scalar couplings. In addition, the use of highly deuterated samples minimizes ^{1}H spin flips that would otherwise exchange multiplet components, leading to potential errors in the estimation of cross-correlation effects. Recently Yang and coworkers have reported a study of relaxation in methyl groups in which cross-correlation between ^{1}H–^{13}C dipolar and ^{13}C CSA mechanisms in methyl groups was quantified using a 3D experiment (Liu et al., 2003), linking the methyl ^{13}C shift of residue i with ^{15}N, HN chemical shifts of residue $i+1$. The experiment described here is significantly more sensitive than this 3D approach, however, resolution can be limiting, especially in applications to large systems.

Figure 2a shows cross-sections from an F_1-coupled ^{1}H–^{13}C CT-HSQC spectrum recorded on protein L with $T = 90$ ms, 5 °C, 800 MHz (correlation time $\tau_c = 10$ ns). In the absence of differential relaxation between the four multiplet components, a 3:1:1:3 quartet is expected. Each of the multiplet components almost always relaxes differently, however, and deviations from a 3:1:1:3 structure are therefore expected. For example, for molecules tumbling in the limit where $\omega_c\tau_c \gg 1$, with ω_c the ^{13}C Larmor frequency (macromolecular limit) and assuming very rapid rotation about the methyl threefold axis, the outer lines relax nine times more rapidly than the inner pair due to cross-correlation between ^{1}H and ^{13}C dipolar interactions (Kay and Torchia, 1991). Further, ^{1}H–^{13}C dipolar/^{13}C CSA cross-correlated relaxation leads to differential relaxation between the outer pair of lines and between the inner components, as well (Vold and Vold, 1978). The net effect is that the multiplet structure observed is one where the components increase in intensity in the direction upfield to downfield (−to + Hz in Figure 2a). The relative intensities of the components depend also on the degree of mobility at a given methyl site. For example, the order parameter describing the amplitude of motions of the methyl averaging axis is significantly smaller for I4δ1 ($S^2_{\text{axis}}\sim 0.4$) than for L56$\delta$2 (0.72), V47$\gamma$2 (0.77) (Millet et al., 2002; Skrynnikov et al., 2002) and the differences in line intensities are therefore less pronounced for the Ile methyl.

The asymmetry in multiplet component intensities can be used to directly provide a measure of ^{1}H–^{13}C dipolar/^{13}C CSA cross-correlated relaxation, η_C, by noting that other relaxation contributions are subtracted when the ratios of outer (inner) intensities are considered. Thus, the ratio of outer (inner) multiplet components is given by $D_{\text{outer}} = \exp(-6\eta_c T)$ ($D_{\text{inner}} = \exp(-2\eta_c T)$), where

$$\eta_C = (-4/15)\, S^2_{\text{axis}} \omega_c \gamma_H \gamma_C \hbar\, (r_{\text{HC}}^{-3}) \tau_c P_2(\cos\beta) \Delta\sigma'_C \tag{1.1}$$

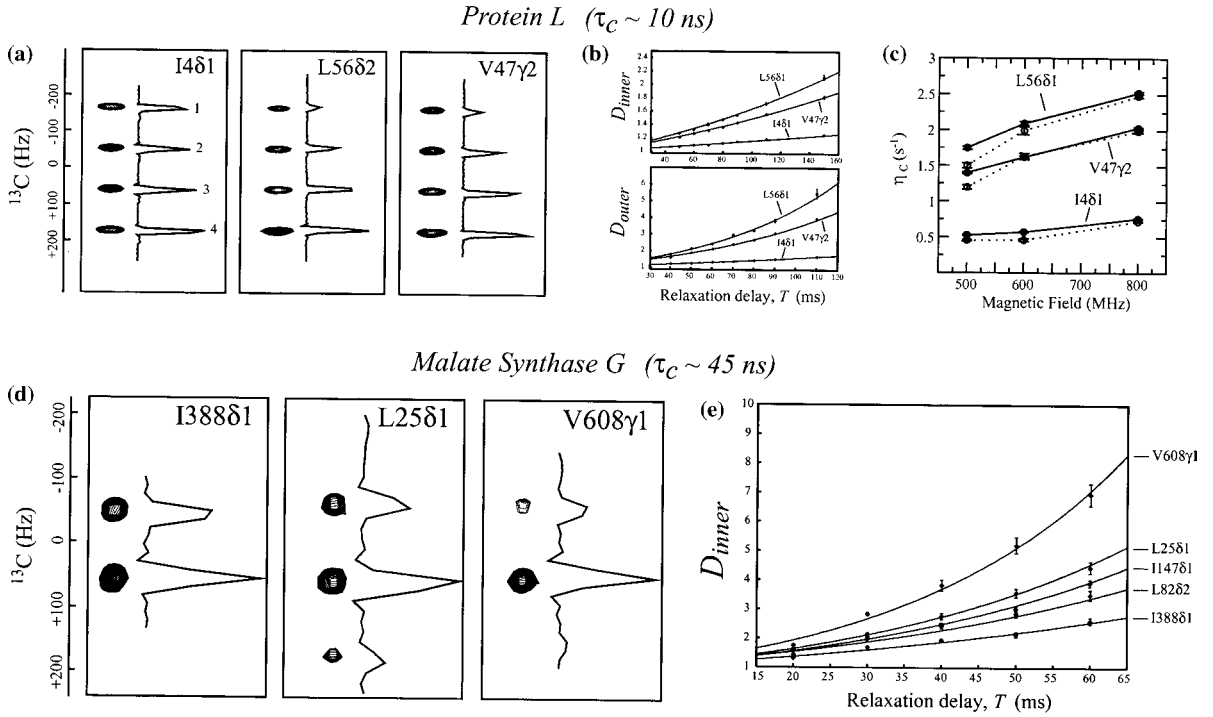

Figure 2. Selected examples of methyl multiplet structures obtained in the F_1 dimension (methyl ^{13}C) of F_1-coupled ^{1}H–^{13}C CT-HSQC spectra, 800 MHz, (pulse scheme of Figure 1a) for (a) protein L and (d) MSG. Exponential build-up curves of the intensity ratios of inner (D_{inner}, lines 2 and 3) and outer (D_{outer}, lines 1 and 4) components for selected methyl groups are shown in (b) for protein L and in (e) for MSG. Panel (c) illustrates the B_o field dependence of methyl ^{1}H–^{13}C dipolar/^{13}C CSA cross-correlation rates (η_C) for I4δ1, L56δ1 and V47γ2 of protein L with solid (dashed) lines corresponding to the rates derived from the outer (inner) multiplet components.

and

$$\Delta\sigma'_C = \{(\sigma_{X,C} - \sigma_{Z,C})P_2(\cos\beta_{X,C}) + (\sigma_{Y,C} - \sigma_{Z,C})P_2(\cos\beta_{Y,C})\}. \quad (1.2)$$

In Equations 1 γ_i is the gyromagnetic ratio of spin i, r_{HC} is the length of the methyl ^{1}H–^{13}C bond, β is the angle between the HC bond and the methyl three fold axis (assumed the C_{methyl}–C axis in what follows), $\beta_{j,C}$ ($j = X,Y$) is the angle between the j principal axis of the ^{13}C CSA tensor and the C_{methyl}–C axis, σ_{iC} ($i = X,Y,Z$) are the principal components of the methyl ^{13}C chemical shielding tensor, $P_2(\cos x) = (3\cos^2 x - 1)/2$ and $\omega_c = \gamma_c B_o$ with B_o the static magnetic field. Equations 1 includes only contributions that are important in the macromolecular limit and considers the case of isotropic overall tumbling of the protein. The value of $P_2(\cos\beta)/(r^3_{HC})$ has been measured to be -0.228 Å^{-3} from ratios of methyl ^{1}H–^{13}C, $^{13}C_{methyl}$–^{13}C dipolar couplings (Ottiger and Bax, 1999; Mittermaier and Kay, 2002).

Values of η_C can be extracted directly from fits of the buildup of D_{outer} and D_{inner} as a function of T, Figure 1b. In Figure 1c η_C values extracted from D_{outer} (solid lines) and D_{inner} (dashed lines) are plotted as a function of magnetic field (a linear dependence is predicted from Equations 1). Values of cross-correlation rates obtained from ratios of inner and outer components are, in general, in good agreement, although deviations as large as 15–20% in rates are noted for measures of η_C obtained at 500 MHz (where the rates are the smallest).

Figure 2d shows cross-sections for a number of residues in MSG obtained from coupled HSQC spectra recorded with $T = 30$ ms, 37 °C, 800 MHz. In this case, the outer components are almost always absent due to efficient ^{1}H–^{13}C dipole–dipole relaxation and values of η_C are extracted from the T dependence of D_{inner}, Figure 2e.

It is clear that it will not be possible to extract all of the relevant CSA parameters listed in

Equations 1 from a single measure, such as η_C. It is, however, possible to obtain estimates for $\Delta\sigma'_C$. Density functional calculations performed on peptide fragments for methyl groups in Ile, Leu and Val, as described in the Materials and methods, establish that to excellent approximation $\Delta\sigma'_C = \Delta\sigma_C P_2(\cos\beta_{Z,C})$, where $\Delta\sigma_C = \sigma_{Z,C} - 1/2(\sigma_{X,C} + \sigma_{Y,C})$, with the Z-axis of the ^{13}C CSA tensor close to collinear with the C_{methyl}–C axis (on average $\beta_{Z,C} = 6.7 \pm 4.8°$). (Note that when $\beta_{Z,C} = 0$ $\Delta\sigma'_C = \Delta\sigma_C$). DFT calculations also establish that $1.0 \le (\Delta\sigma_C/\Delta\sigma'_C) \le 1.1$ and that $(\Delta\sigma_C/\Delta\sigma'_C)_{avg} = 1.03 \pm 0.03$; that is $\Delta\sigma_C \sim \Delta\sigma'_C$. Reasonable estimates of the methyl carbon CSA can therefore be obtained from η_C so long as values for S^2_{axis} and τ_c are known.

Average values for $\Delta\sigma_C$ can be calculated for Ile (δ1), Leu and Val methyls in protein L since methyl axis order parameters have been measured previously from ^2H spin relaxation measurements (Skrynnikov et al., 2002). Protein L does not tumble isotropically, ($D_{//}/D_{\perp} = 1.35$); assuming that the structure of the protein in solution is rigid and identical to the X-ray structure, the effect of anisotropic tumbling on computed values of $\Delta\sigma_C$ can be estimated using the orientation of each C_{methyl}–C axis with respect to the diffusion frame of the molecule (Skrynnikov et al., 2002). Computations establish that the effects of diffusion anisotropy change the extracted CSA values by less than 5%. Because many of the methyl groups are dynamic it is unlikely that their average orientation is properly described by the X-ray structure and we have chosen, therefore, to use an isotropic correlation time in the analysis. Values of 18.2 ± 1.5 (15.6 ± 3.6), 25.8 ± 5.6 (23.8 ± 5.5) ppm are calculated for $\Delta\sigma_C$ for Ile (δ1) and Leu/Val, respectively, from η_C values measured from the time evolution of the outer (inner) lines. (Values for Leu and Val are essentially the same and we have thus averaged them.) By comparison, $\Delta\sigma_C = 22.6 \pm 4.9$ and 35.2 ± 4.5 ppm are obtained for Ile (δ1) and Leu/Val from DFT calculations along with asymmetries, $1.5|(\sigma_{Y,C}\text{-}\sigma_{X,C})/\Delta\sigma_C|$, of 0.6 ± 0.1 (Ile) and 0.4 ± 0.1(Leu/Val), while $\Delta\sigma_C$ values of 17 ± 8, 30 ± 6, 23 ± 8 ppm have been measured from solid state NMR studies of powders of the amino acids Ile (δ1), Leu and Val (Ye et al., 1993). Recently, Ishima and coworkers have reported methyl ^{13}C $\Delta\sigma$ values of 14.3 ± 0.3, 26.7 ± 3.4 and 27.1 ± 4.6 ppm measured by solid state NMR studies of dipeptides of Gly-Ile, Gly-Leu and Gly-Val, respectively (Ishima et al., 2001). Thus, the ^{13}C CSA values that have been obtained in the present work fall within the range of values measured using more 'conventional' methodologies, although they are somewhat smaller than those predicted by DFT. It is worth noting that a similar analysis of $\Delta\sigma_C$ values from measurements on MSG must await the determination of S^2_{axis} for each of the methyl groups in this protein.

Cross-correlated relaxation interference of ^1H–^{13}C dipolar/^1H CSA interactions has also been measured for Ile (δ1), Leu and Val $^{13}CH_3$ groups in protein L and MSG, Figure 1b. An F_2-coupled HMQC pulse scheme has been used in which evolution from relaxation interactions including the cross-correlation of interest is allowed to occur during a delay T' in the sequence prior to acquisition. A purge element of duration $2\zeta = 1/(4J_{HC})$, where J_{HC} is the one-bond ^1H–^{13}C scalar coupling constant, has been included in the scheme of Figure 1b to ensure that the detected signal is derived from only the slowly relaxing pathway of magnetization transfer during the sequence (Tugarinov et al., 2003; Korzhnev et al., 2004). For proteins such as MSG ($\tau_c = 45$ ns, 37 °C) this will almost certainly be the case even in the absence of the purge element, but for protein L ($\tau_c = 10$ ns, 5 °C) insertion of the purge ensures that the decay of each ^1H multiplet component during T', is single exponential (Tugarinov et al., 2003).

A series of spectra were acquired as a function of delay T', Figure 3a (protein L), c (MSG) and the intensity vs. T' profile of each of the doublet components fit to an exponential function to extract relaxation rates of each of the lines, Figure 3b, d; the dipole/CSA cross-correlation rate, η_H is given by $0.5(R_{2u} - R_{2d})$, where R_{2u}, R_{2d} are the relaxation rates of the upfield and downfield ^1H lines, respectively. Notably, in the majority of cases multiplet components increase from upfield to downfield, as in ^{13}C CSA measurements, implying that η_H and η_C have the same sign.

Measured values of η_H depend on the principal components of the ^1H CSA tensors of each of the three methyl protons according to

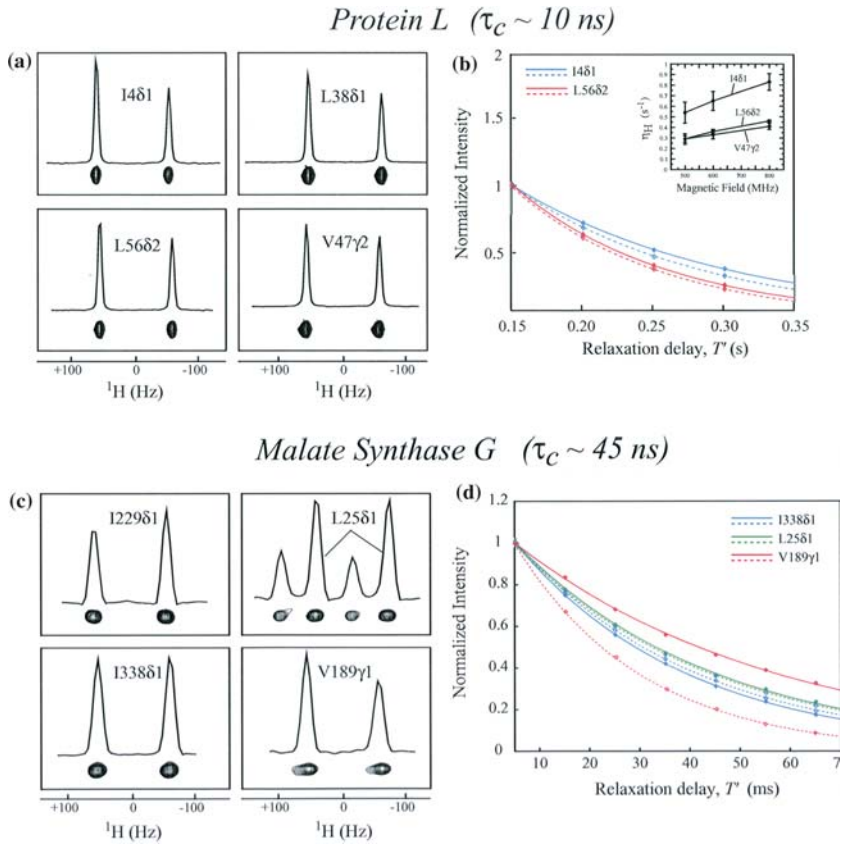

Figure 3. Typical examples of the methyl doublet structure obtained in the acquisition (methyl ^{1}H) dimension using the pulse scheme of Figure 1b, 800 MHz, for selected residues of (a) protein L and (c) MSG. Exponential decay curves of the two doublet lines belonging to the same methyl group in protein L (b) and MSG (d) are shown with the same colors using solid (dashed) lines for downfield (upfield) components. The inset in (b) illustrates the approximately linear B_o field dependence of the measured methyl ^{1}H–^{13}C dipolar/^{1}H CSA cross-correlation rates (η_H) for I4δ1, L56δ2 and V47γ2 methyl groups of protein L.

$$\eta_H = (-4/15) S^2_{\text{axis}} \omega_H \gamma_H \gamma_C \hbar (r^{-3}_{\text{HC}}) \tau_c P_2(\cos\beta) \Delta\sigma'_H, \tag{2.1}$$

$$\Delta\sigma'_H = (1/3)\Sigma_i \{(\sigma_{X,Hi} - \sigma_{Z,Hi}) P_2(\cos\beta_{X,Hi}) + (\sigma_{Y,Hi} - \sigma_{Z,Hi}) P_2(\cos\beta_{Y,Hi})\}, \tag{2.2}$$

where the summation in Equation 2.2 is over the three methyl protons, $i = 1$–3, $\sigma_{A,\text{H}i}$ is the $A = (X,Y,Z)$ component of the principal CSA tensor of proton i and $\beta_{A,\text{H}i}$ is the angle that the A CSA axis makes with respect to the C_{methyl}–C bond. The derivation of Equations 2 is based on the assumption that methyl rotation is governed by a three fold degenerate potential so that the summation is over the three equiprobable orientations of the methyl ^{1}H–^{13}C vector. The relation between Equations 1 and 2 can be made more transparent by noting that

$$\Delta\sigma'_H = \{(\sigma_{X,\text{Havg}} - \sigma_{Z,\text{Havg}}) P_2(\cos\beta_{X,\text{Havg}}) + (\sigma_{Y,\text{Havg}} - \sigma_{Z,\text{Havg}}) P_2(\cos\beta_{Y,\text{Havg}})\}, \tag{3}$$

where $\sigma_{A,\text{Havg}}$ is the principal value of the A component of the *averaged* CSA tensor and $\beta_{A,\text{Havg}}$ is the angle of the A principal axis of the averaged tensor with respect to the C_{methyl}–C axis. It is not possible to extract individual averaged ^{1}H chemical shielding tensor elements from a single measured cross-correlation relaxation rate, but rather $\Delta\sigma'_{\text{H}}$ (which is three fold averaged). DFT calculations of methyl ^{1}H

chemical shift tensors in ubiquitin show that to excellent approximation

$$\Delta\sigma'_H = \{\sigma_{Z,\mathrm{Havg}} - 1/2(\sigma_{X,\mathrm{Havg}} + \sigma_{Y,\mathrm{Havg}})\}P_2(\cos\beta_{Z,\mathrm{Havg}}). \quad (4)$$

Note that in the limit where the averaged methyl CSA tensor is axially symmetric Equation 4 is an identity. The DFT computations establish that the left and right hand sides of Equation 4 deviate by 2% on average (based on 11 methyl groups) with a standard deviation of 13%. Notably, unlike the Z-axis of the methyl ^{13}C CSA tensor which is nearly collinear with the C_{methyl}–C bond, DFT calculations indicate that $\beta_{Z,\mathrm{Havg}} = 25 \pm 9°$, so that what is obtained from analysis of η_H values is the effective rank-2 projection of the ^{1}H CSA tensor on the methyl three fold axis, Eq 4. Values of $\Delta\sigma'_H = 1.1 \pm 0.7$ ppm are extracted from measurements of η_H in protein L, based on data from 15 Ile (δ1), Leu, Val methyls.

In order to increase the data base of $\Delta\sigma'_H$ values beyond those that are available from protein L we have calculated $\Delta\sigma'_H$ for MSG using an approach which combines measurements of η_C and η_H. Recall that for this protein values of S^2_{axis} are not available and it is therefore not possible to obtain $\Delta\sigma'_H$ directly from η_H. However, it is possible to isolate $\Delta\sigma'_H$ from the ratio η_C/η_H, assuming that values for $\Delta\sigma_C$ are available, since $\eta_C/\eta_H = (\omega_C\Delta\sigma_C)/(\omega_H\Delta\sigma'_H)$. In what follows we have used $\Delta\sigma_C = 18$ and 25 ppm, for Ile (δ1) and Leu/Val methyl carbons, respectively. Figure 4 shows the distribution of $\Delta\sigma'_H$ values that have been obtained in this manner with an average $\Delta\sigma'_H$ of 1.1 ± 1.0 ppm (the distribution also contains CSA values from protein L, calculated in the same manner as for MSG). Although the bulk of the $\Delta\sigma'_H$ values are positive, for several residues negative values are measured. This is clear for I229 (δ1) of MSG where the intensities of the multiplet components are reversed relative to the majority of residues in the protein, Figure 3c.

Unlike the case for carbon where methyl CSA values from several experimental studies are available, to our knowledge only a single solid state NMR study has been published that reports ^{1}H CSA values of methyl groups in a compound that is at least 'similar' in structure to an amino acid (most of the tabulated data pertain to halogenated methyls). Haeberlen and coworkers have

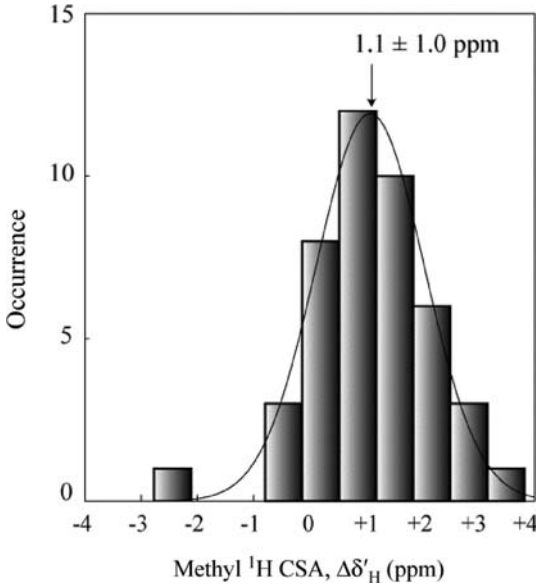

Figure 4. Histogram of methyl ^{1}H CSA values derived from the analysis of η_C and η_H cross-correlation rates in MSG and protein L. ^{1}H CSA values obtained from the two proteins (29 and 15 methyls in MSG and Protein L, respectively) are combined and the distribution fit to a Gaussian function of mean value of 1.1 ppm and standard deviation 1.0 ppm.

measured $\Delta\sigma_{\mathrm{Havg}} = 1.6 \pm 0.2$ ppm for dimethylmalonic acid and show that, at least in this compound, the chemical shielding tensor is axially symmetric (Scheubel et al., 1988). In addition, the Z-axes of the ^{13}C and ^{1}H CSA tensors are within 10° of each other in this molecule. The $\Delta\sigma_{\mathrm{Havg}}$ value reported for dimethylmalonic acid (Scheubel et al., 1988) is similar to values measured here from spin relaxation studies. Of interest, the values of $\Delta\sigma_{\mathrm{Havg}}$ that have been calculated from DFT computations are 2–2.5 fold larger than what has been measured experimentally; the relatively large factor is mainly due to the small size of the ^{1}H methyl anisotropies. In addition, it may also reflect the inherent difficulties with computations involving protons (Malkin et al., 1994, 1995b).

In summary, simple pulse schemes are presented for providing estimates of ^{13}C and ^{1}H methyl CSA values from measurements of dipole/CSA cross-correlated spin relaxation rates. Measurements of ^{13}C CSA values for Ile (δ1), Leu and Val methyls in protein L and in MSG are in good agreement with values obtained from solid state NMR studies and in reasonable agreement with values computed by DFT. The present

study significantly enlarges the database of proton methyl anisotropies; $\Delta\sigma'_H$ values obtained are small, on average 1 ppm.

Acknowledgements

This work was supported by a Grant from the Canadian Institutes of Health Research to L.E.K. and from the NSF (NCB–0211512) to R. B. V.T. acknowledges the support of the Human Frontiers Science Program. L.E.K. holds a Canada Research Chair in Biochemistry.

References

Ahlrichs, R. and Arnim, M. (1995) In *Methods and Techniques in Computational Chemistry: METECC-95*, Clementi, E. and Corongiu, G. (Eds.).

Ahlrichs, R., Bär, M., Häser, M., Horn, H. and Kölmel, C. (1989) *Chem. Phys. Lett.*, **162**, 165.

Cornilescu, G., Marquardt, J., Ottiger, M. and Bax, A. (1998) *J. Am. Chem. Soc*, **120**, 6836–6837.

Delaglio, F., Grzesiek, S., Vuister, G. W., Zhu, G., Pfeifer, J. and Bax, A. (1995) *J. Biomol. NMR*, **6**, 277–293.

Duncan, T.M. (1990) *A Compilation of Chemical Shift Anisotropies*, The Farragut Press, Chicago.

Gardner, K.H. and Kay, L.E. (1997) *J. Am. Chem. Soc.*, 119, 7599–7600.

Gardner, K.H., Rosen, M.K. and Kay, L.E. (1997) *Biochemistry*, **36**, 1389–1401.

Gardner, K.H., Zhang, X., Gehring, K. and Kay, L.E. (1998) *J. Am. Chem. Soc.*, **120**, 11738–11748.

Godbout, N., Salahub, D.R., Andzelm, J. and Wimmer, E. (1992) *Can. J. Chem.*, **70**, 560–571.

Goto, N.K., Gardner, K.H., Mueller, G.A., Willis, R.C. and Kay, L.E. (1999) *J. Biomol. NMR*, **13**, 369–374.

Howard, B.R., Endrizzi, J.A. and Remington, S.J. (2000) *Biochemistry*, **39**, 3156–3168.

Ishima, R., Petkova, A.P., Louis, J.M. and Torchia, D.A. (2001) *J. Am. Chem. Soc.*, **123**, 6164–6171.

Kay, L.E. and Bull, T.E. (1992) *J. Magn. Reson.*, **99**, 615–622.

Kay, L.E. and Prestegard, J.H. (1987) *J. Am. Chem. Soc.*, 3829–3835.

Kay, L.E., and Torchia, D.A. (1991) *J. Magn. Reson.*, **95**, 536–547.

Kay, L.E., Bull, T.E., Nicholson, L.K., Griesinger, C., Schwalbe, H., Bax, A. and Torchia, D.A. (1992) *J. Magn. Reson.*, **100**, 538–558.

Korzhnev, D.M., Kloiber, K., Kanelis, V., Tugarinov, V. and Kay, L.E. (2004) *J. Am. Chem. Soc.*, **126**, 3964–3973.

Kroenke, C.D., Loria, J.P., Lee, L.K., Rance, M. and Palmer, A.G. (1998) *J. Am. Chem. Soc.*, **120**, 7905–7915.

Kutzelnigg, W., Fleischer, U. and Schindler, M. (1991) In *NMR: Basic Principles and Progress*, Diehl, P., Fluck, E. and Kosfeld, E. (Eds.), Springer, Berlin, pp. 165–262.

Levitt, M. and Freeman, R. (1978) *J. Magn. Reson.*, **33**, 473–476.

Liu, W., Zheng, Y., Cistola, D.P. and Yang, D. (2003) *J. Biomol. NMR*, **27**, 351–364.

Malkin, V.G., Malkina, O.L., Casida, M.E. and Salahub, D.R. (1994) *J. Am. Chem. Soc.*, **116**, 5898–5908.

Malkin, V.G., Malkina, O.L., Eriksson, L.A. and Salahub, D.R. (1995a) In *Modern Density Functional Theory: A Tool for Chemists*, Seminario, J.M. and Politzer, P. (Eds.), Elsevier, Amsterdam.

Malkin, V.G., Malkina, O.L. and Salahub, D.R. (1995b) In *Theoretical and Computational Chemistry*, Seminario, J.M. and Politzer, P. (Eds.), Elsevier, Amsterdam.

Malkin, V.G., Malkina, O.L. and Salahub, D.R. (1996) *Chem. Phys. Lett.*, **261**, 335–345.

Marion, D., Ikura, M., Tschudin, R. and Bax, A. (1989) *J. Magn. Reson.,* **85**, 393.

Metzler, W.J., Wittekind, M., Goldfarb, V., Mueller, L. and Farmer, B.T. (1996) *J. Am. Chem. Soc.*, **118**, 6800–6801.

Millet, O., Muhandiram, D.R., Skrynnikov, N.R. and Kay, L.E. (2002) *J. Am. Chem. Soc.,* **124**, 6439–6448.

Mittermaier, A. and Kay, L.E. (1999) *J. Am. Chem. Soc.*, **121**, 10608–10613.

Mittermaier, A. and Kay, L.E. (2002) *J. Biomol. NMR*, **23**, 35–45.

Mueller, G.A., Choy, W.Y., Yang, D., Forman-Kay, J.D., Venters, R.A. and Kay, L.E. (2000) *J. Mol. Biol.*, **300**, 197–212.

Muhandiram, D.R., Yamazaki, T., Sykes, B.D. and Kay, L.E. (1995) *J. Am. Chem. Soc.*, **117**, 11536–11544.

Muller, N., Bodenhausen, G. and Ernst, R.R. (1987) *J. Magn. Reson.*, **75**, 297–334.

Ollerenshaw, J.E., Tugarinov, V. and Kay, L.E. (2003) *Magn. Reson. Chem.*, **41**, 843–852.

Ottiger, M. and Bax, A. (1999) *J. Am. Chem. Soc.*, **121**, 4690–4695.

Palmer, A.G., Wright, P.E., and Rance, M. (1991) *Chem. Phys. Lett.,* **185**, 41–46.

Perdew, J.P. and Wang, Y. (1992) *Phys. Rev. B*, **45**, 13244–13249.

Richarz, R., Nagayama, K. and Wüthrich, K. (1980) *Biochemistry*, **19**, 5189–5196.

Rosen, M.K., Gardner, K.H., Willis, R.C., Parris, W.E., Pawson, T. and Kay, L.E. (1996) *J. Mol. Biol.*, **263**, 627–636.

Salahub, D.R., Fournier, R., Mlynarski, P., Papai, I., St-Amant, A. and Ushio, J. (1991) In *Density Functional Methods in Chemistry*, Labanowski, A. and Andzelm, J. (Eds.), Springer, New York, p. 77.

Santoro, J. and King, G.C. (1992) *J. Magn. Reson.*, **97**, 202–207.

Scalley, M.L., Yi, Q., Gu, H., McCormack, A., Yates, J.R. and Baker, D. (1997) *Biochemistry*, **36**, 3373–3382.

Scheubel, W., Zimmerman, H. and Haeberlen, U. (1988) *J. Magn. Reson.*, **80**, 401–416.

Scheurer, C., Skrynnikov, N.R., Lienin, S.F., Straus, S.K., Brüschweiler, R. and Ernst, R.R. (1999) *J. Am. Chem. Soc.*, **121**, 4242–4251.

Shaka, A.J., Keeler, J., Frenkiel, T. and Freeman, R. (1983) *J. Magn. Reson.*, **52**, 335–338.

Skrynnikov, N.R., Millet, O. and Kay, L.E. (2002) *J. Am. Chem. Soc.*, **124**, 6449–6460.

Sosa, C., Andzelm, J., Elkin, B.C., Wimmer, E., Dobbs, K.D. and Dixon, D.A. (1992) *J. Phys. Chem.*, **96**, 6630–6636.

Tjandra, N. and Bax, A. (1997a) *J. Am. Chem. Soc.*, **119**, 9576–9577.

Tjandra, N. and Bax, A. (1997b) *J. Am. Chem. Soc.*, **119**, 8076–8082.

Tugarinov, V. and Kay, L.E. (2003a) *J. Am. Chem. Soc.*, **125**, 13868–13878.
Tugarinov, V. and Kay, L.E. (2003b) *J. Biomol. NMR*, **28**, 165–172.
Tugarinov, V. and Kay, L.E. (2004) *J. Biomol. NMR*, **29**, 369–376.
Tugarinov, V., Hwang, P.M., Ollerenshaw, J.E., and Kay, L.E. (2003) *J. Am. Chem. Soc.*, **125**, 10420–10428.
Tugarinov, V., Muhandiram, R., Ayed, A. and Kay, L.E. (2002) *J. Am. Chem. Soc.*, **124**, 10025–10035.
Vold, R.L. and Vold, R.R. (1978) *Prog. NMR Spectrosc.*, **12**, 79–133.
Vuister, G.W. and Bax, A. (1992) *J. Magn. Reson.*, **98**, 428–435.
Werbelow, L.G. and Grant, D.M. (1977) *Adv. Magn. Reson.*, **9**, 189–299.
Werbelow, L.G. and Marshall, A.G. (1973) *J. Magn. Reson.*, 299–313.
Ye, C., Fu, R., Hu, J., Hou, L. and Ding, S. (1993) *Magn. Reson. Chem.*, **31**, 699–704.